JOURNAL OF MATERIALS SCIENCE 25 (1990) 4785–4791

Microstructural development in non-oriented lamination steels

Part IV *The effect of cold rolling and annealing*

J-W. LEE*, P. R. HOWELL
Department of Materials Science and Engineering, The Pennsylvania State University, University Park, Pennsylvania 16802, USA

The effect of cold rolling and annealing on the structure of two lamination steels has been examined using scanning electron microscopy and transmission electron microscopy. It is demonstrated that the massive films of cementite (which are a characteristic of the hot rolled strip) are fragmented during cold rolling. Fracture of the massive films occurred in a brittle manner. Smaller cementite precipitates did not fail by brittle cracking but sometimes necked down leading to ductile failure. Annealing in either the two-phase ferrite plus cementite, or ferrite plus austenite regions led to the gradual development of cavities. It is likely that these cavities grew by the short-circuit diffusion of excess vacancies driven by pre-strains.

1. Introduction

The relatively low cost of low carbon steels often justifies their use in magnetic applications in a laminated form. Since the microstructures of the steels are closely associated with the resulting textures, which in turn can affect the magnetic properties of these materials, it is necessary to bring the process parameters under close control and to gain a fundamental understanding of the microstructural changes accompanying processing, thus, as a part of an overall study concerning the affect of processing on microstructures, the effect of cold rolling and annealing on the structure of two hot rolled low carbon steels has been examined.

In a study of temper rolled steels by the present authors [1], cavities were observed at cementite–ferrite interfaces, and to our knowledge, this was the first report of cavitation in lamination steels. Although the exact details of the processing were not available, the formation of the cavities was postulated to occur as follows:

(1) during cold rolling, cracks occurred at the interface between ferrite and cementite due to the development of stress concentrations and

(2) the cracks developed into cavities during subsequent annealing by the acquisition of excess vacancies which were generated by the cold rolling.

In order to more fully understand the formation of cavities, the present investigation was initiated. Specimen materials in the form of hot rolled strips were deformed by cold rolling to various strains and subsequently annealed, both in the two-phase ferrite plus cementite and in the two-phase ferrite plus austenite region. The major objectives of this investigation are as follows.

(1) To document the microstructural changes which occur during rolling and subsequent annealing.

(2) To correlate the formation of cavities during annealing with the distribution of cracks in the rolled material.

(3) To investigate the mechanisms of crack and cavity formation.

2. Experimental procedures

Specimen materials in the as-received hot rolled condition (2.5 mm thick strip) were obtained from Inland Steel in Chicago. The chemical compositions of the two steels are given in Table I.

To determine the effect of cold rolling and annealing (and to simulate the processing schedule of the temper rolled steels [1]), hot rolled specimens were cold rolled in the laboratory to reductions in thickness in the range of 10 to 70%. Subsequently, cold rolled specimens (70% reduction) were annealed at either 700° C (in the two phase ferrite plus cementite region) or at 740° C (in the two phase austenite plus ferrite region). In both cases, the specimens were furnace cooled after annealing.

Specimens for scanning electron microscopy (SEM) were prepared using standard metallographic techniques and etched in 2% nital. SEM examinations were conducted on an ISI Super IIIA using an accelerating potential of 25 kV. Specimens for transmission

TABLE I Chemical compositions and experimental materials

	C	Mn	Si	P	S	Al	N
Hot rolled steel A	0.04	0.6	0.05	0.06	0.02	< 0.008	–
Hot rolled steel B	0.04	0.7	0.22	0.09	0.02	0.21	–

* *Present address*: Department of Metallurgical Engineering and Materials Science, Carnegie-Mellon University, Pennsylvania 15213, USA.

0022–2461/90 $03.00 + .12

electron microscopy (TEM) were prepared in a twin-jet electropolisher using an electrolyte consisting of 5% perchloric acid in glacial acetic acid at 298 K and at a potential of 35 V. TEM was performed using a Philips EM 300 operating at 100 kV.

3. Results

3.1. The structure of the hot rolled specimen materials

The hot rolled steels which were used in this investigation exhibited the following microstructural characteristics:

(i) approximately equiaxed lamellar pearlite colonies together with proeutectoid ferrite and

(ii) massive films of cementite both at ferrite grain boundaries and at ferrite–pearlite interfaces.

In the following, the microstructural changes which were effected, by both cold rolling and annealing, are documented. Further details concerning the nature of the hot rolled steels are given in Lee and Howell [2].

3.2. The structure of the cold rolled specimen materials

3.2.1. The effect of cold rolling on the massive films of cementite at ferrite grain boundaries

Figs 1 and 2 are SEM micrographs of steel A after 70 and 50% reduction, respectively. In Fig. 1, the continuous film of cementite at the ferrite grain boundary has been fragmented by brittle cracking (arrowed A). The cracks are restricted primarily to the films and do not extend appreciably into the surrounding ferrite. These observations imply that the cracks nucleate at the ferrite–cementite interfaces. Similarly, Fig. 2 shows brittle cracking associated with a massive grain boundary film of cementite (arrowed A). Cavitation has occurred between fragmented cementite precipitates (arrowed B on Fig. 2) and at the ferrite–cementite interface (arrowed C on Fig. 2). However, it should be noted that the smaller and discrete cementite precipitates have not fragmented (arrowed D on Fig. 2).

Decreasing the percentage reduction leads to a reduction in the number of cracks but little change in the crack mode. Figs 3 and 4 are from steel B (20 and 10% reduction, respectively). These figures show grain boundary cementite films which exhibit ductile necking and cracking (A on Figs 3 and 4). Ductile failure was only observed for relatively thin cementite films and brittle cracks were still observed at massive films of cementite, even for low percentage reductions. In comparing the two steels, it was found that brittle cracking was more prevalent in steel A than in steel B. This is consistent with the observation that massive films of cementite were a more frequent occurrence in steel A [2].

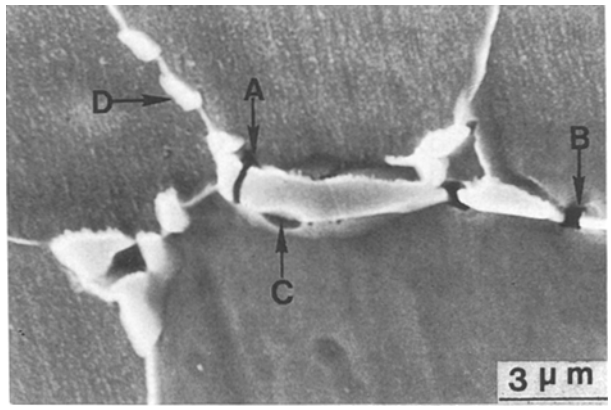

Figure 2 SEM image of cracks (A) and cavities (B and C) which are associated with cementite precipitates. Note that small and discrete precipitates are not cracked (D) (50% reduction, steel A).

3.2.2. The affect of cold rolling on the pearlite colonies

Figs 5 and 6 show cracks and cavities which are associated with pearlite colonies. In both instances brittle cracks are associated with massive cementite films at the pearlite–ferrite interfaces (arrowed A on the figures). For a reduction of 70% (Fig. 5, steel B), extensive cracking of the pearlitic cementite also occurred (arrowed B). Consideration of Fig. 5 suggests that the fracture of the cementite lamellae occurred by shear cracking. It should also be noted that cavitation occurs within the pearlitic ferrite at the ferrite–cementite interface (arrowed C and D). In Fig. 6 (50% reduction, steel A), the cracks which are associated with the cementite film at the ferrite–pearlite interface (arrowed A and B) have advanced into the pearlite colony, resulting in cracking of the cementite lamellae (arrowed C). This implies that the cracks observed within pearlite colonies originate from fractured cementite films. In common with the observations

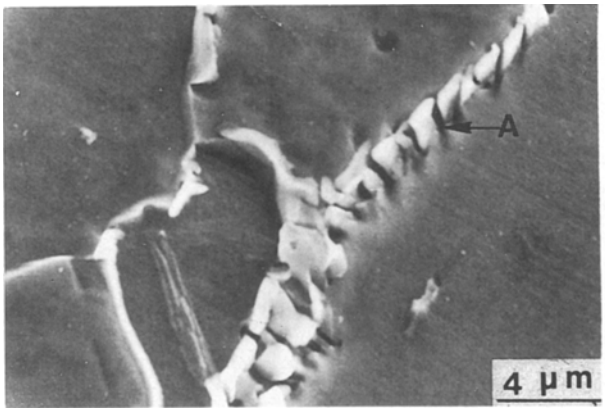

Figure 1 SEM image of brittle cracks (A) at a grain boundary film of cementite after 70% reduction (steel A).

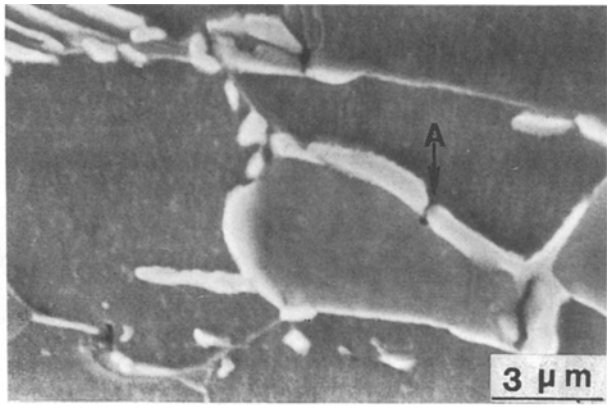

Figure 3 Ductile cracking (A) of a thin film of cementite (20% reduction of hot rolled steel B).

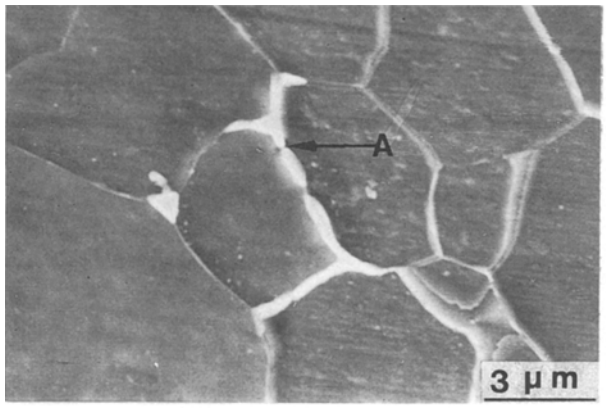

Figure 4 SEM image of a fractured cementite film after 10% reduction showing ductile failure of thin cementite precipitate (arrowed A, steel B).

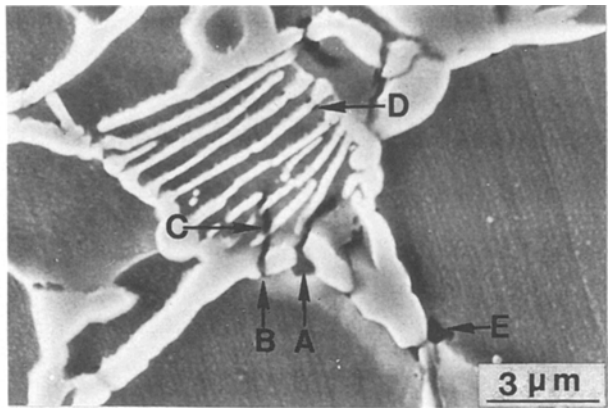

Figure 6 SEM image of cracks (A, B) and cavities (D, E) after 50% reduction. Note that a crack in a massive film of cementite at a pearlite–ferrite interface has advanced into the pearlite (steel A).

made with respect to Fig. 5, cavities in the ferrite, both at pearlitic ferrite–cementite interfaces (arrowed D), and at proeutectoid ferrite–grain boundary cementite interfaces (arrowed E), are also observed.

A decrease in the percentage reduction leads to a lower frequency of occurrence of brittle cracking of the cementite films at ferrite–pearlite interfaces as is shown in Figs 7 and 8 (which were recorded from specimen material deformed by 30 and 20%, respectively). In Fig. 7, the formation of small cavities in the ferrite at the ferrite–grain boundary cementite film interface is associated with necking of the film (arrowed B). Fig. 8 shows that for this level of deformation (i.e., 20%), the cracks do not propagate into the pearlite. For the lowest level of deformation (10%), no cracking of the thin cementite at the pearlite–ferrite interfaces occurred, however, cracks and cavities were observed at pearlite–massive cementite film interfaces.

A TEM examination of specimen material cold rolled to 20% reduction revealed the initiation of an ill formed deformation substructure in the ferrite matrix. With an increase in percentage reduction, this substructure became a continuous network dividing the ferrite into separate subgrains. These cells tended to be elongated along the rolling direction.

Occasionally, kinking of the cementite lamellae was observed (Fig. 9, 20% reduction). This implies that cementite lamellae can be plastically deformed and that compressive stresses are operative during cold rolling [3].

3.2.3. Summary

The results presented in this section can be summarized as follows.

(1) As the percentage reduction increases, the frequency of occurrence of cracks increases.

(2) Extensive brittle cracking occurs at massive films of cementite, both at ferrite grain boundaries and at pearlite–ferrite interfaces for all percentage reductions.

(3) Thin and discrete cementite precipitates do not exhibit brittle fracture, however, some of the thin cementite films do neck down, resulting in ductile cracking.

(4) The propagation of cracks into the ferritic matrix is very limited.

(5) Cracking is more prevalent in steel A than in steel B and no cracks are seen in the absence of cementite.

3.3. The affect of annealing on the structure of cold rolled specimen materials

After annealing, a pronounced change in the morphology of the fractured cementite and the cracks occurred. Figs 10 to 12 are SEM micrographs of steel A (Figs 10 and 11) and steel B (Fig. 12) which had been cold rolled by 70% and annealed at 700° C for 5 min. Recrystallization of the deformed ferrite is complete at this stage as is evinced by the fractured

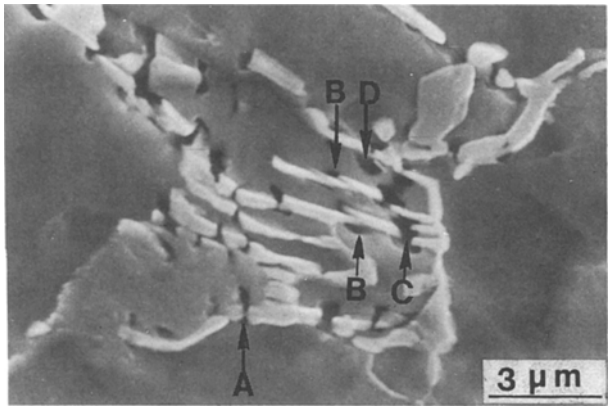

Figure 5 SEM image of shear cracking in a pearlite colony (arrowed B). Note that brittle cracking (arrowed A) and cavitation (arrowed B, C and D) has occurred (70% reduction, steel B).

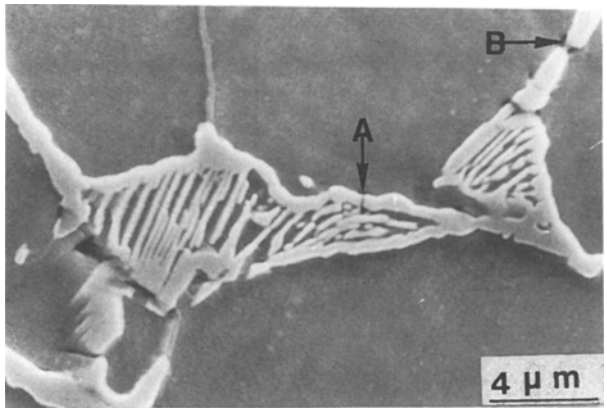

Figure 7 Cracks at pearlite–ferrite (A) and ferrite–ferrite (B) interfaces after 30% reduction (steel A).

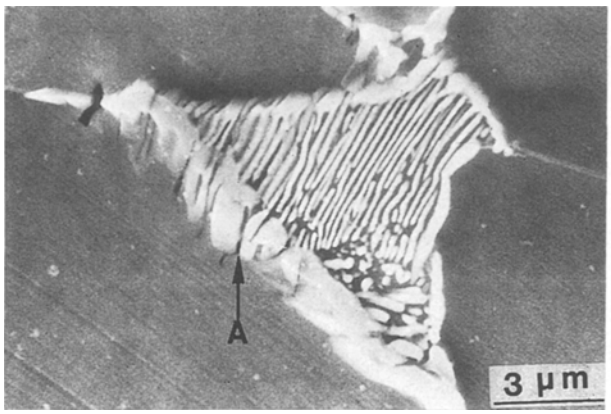

Figure 8 SEM image of cementite cracks at pearlite–ferrite interfaces (A) after 20% reduction (steel A).

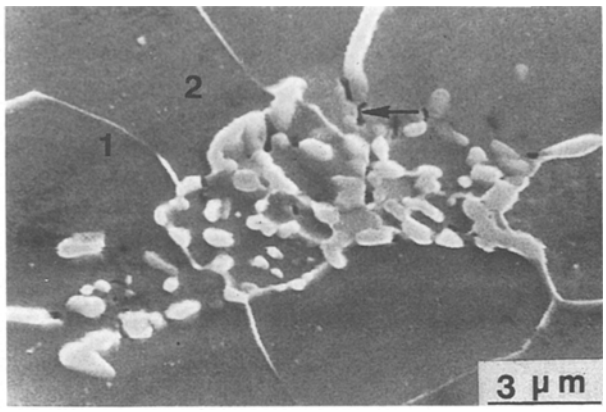

Figure 11 A pearlite colony lying across ferrite grains 1 and 2 (70% cold rolling plus annealing for 5 min at 700° C, steel A).

Figure 9 Kinking of cementite lamellae in a pearlite colony after 20% reduction (steel B).

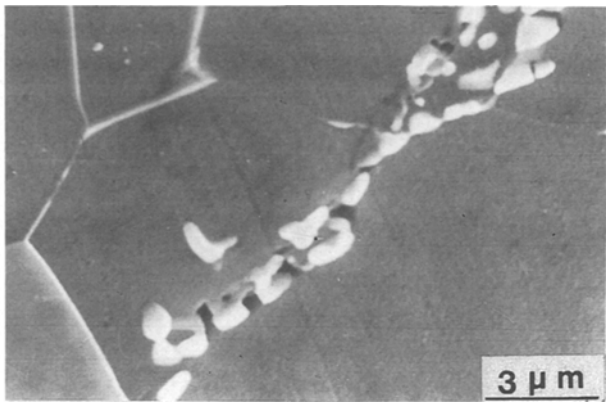

Figure 12 Cavities and cracks in association with an isolated film of cementite (70% cold rolling plus annealing for 5 min at 700° C, steel B).

pearlite colonies lying across e.g., ferrite grains 1 and 2 in Figs 10 and 11. In addition, the cementite appears to be partially spheroidized whilst the cracks have also spheroidized partially (arrowed in Fig. 11) and pre-existing cavities have coarsened. Spheroidization of the cementite reduces the interfacial free energy and is most probably accelerated by recrystallization (Section 4.2). Similarly, spheroidization of the pre-existing cracks and cavities may be due to the growth of the cavities by excess vacancies which were generated by cold rolling.

Increasing the annealing time (25 min at 700° C) resulted in considerable spheroidization of the cementite and the vast majority of the cracks developed into cavities as is shown in Figs 13 and 14 (steel A) and 15 (steel B). In many instances, isolated cavities (arrowed on Figs 13 and 15) were observed in the absence of cementite. This can be explained by the coarsening of cementite which can lead to dissolution of the smaller precipitates. In addition, spheroidization of the cavities is more extensive. Again, recrystallization of the ferrite has produced "pearlite colonies" which traverse several

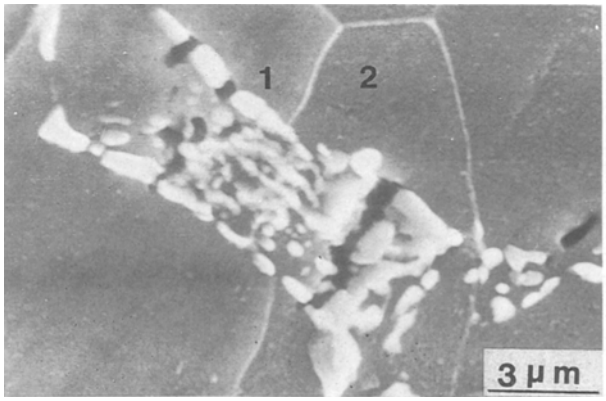

Figure 10 SEM image of a pearlite colony lying across ferrite grains 1 and 2 after annealing (70% cold rolling, plus annealing for 5 min at 700° C, steel A).

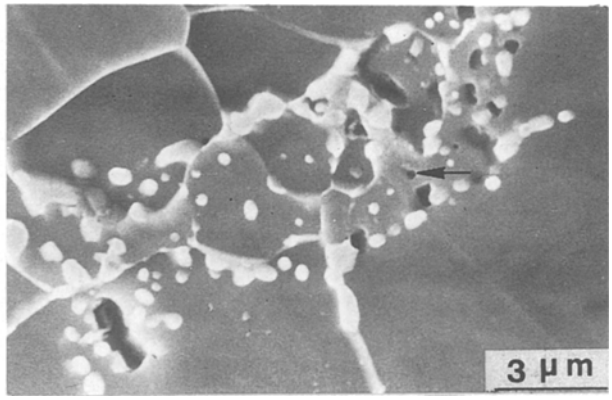

Figure 13 Spheroidization of fractured cementite and growth of cavities from cracks (70% cold rolling plus annealing for 25 min at 700° C, steel A).

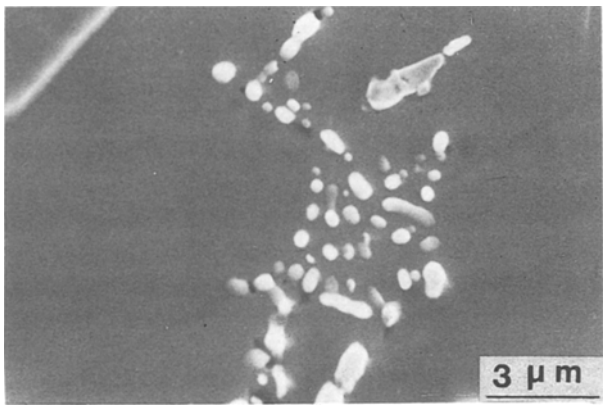

Figure 14 An isolated pearlite colony (70% cold rolling plus annealing for 5 min at 700° C, steel B).

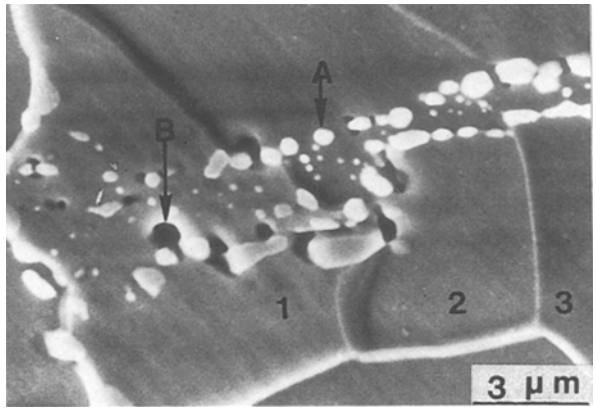

Figure 16 Spheroidization of fractured cementite and growth of cavities from cracks (70% cold rolling plus annealing for 3 min at 740° C, steel A).

ferrite grains (Fig. 13) and in Fig. 14, the "pearlite colony" is isolated within the ferrite matrix.

Figs 16 and 17 are microstructures developed after deforming by 70% prior to annealing at 740° C for 3 min. Spheroidization of fractured cementite (arrowed A) and the development of cavities (arrowed B) is more complete compared with the structures developed at 700° C after 5 min annealing (see Figs 10 to 12). In common with the anneal at 700° C, recrystallization is complete after 3 min at 740° C and single pearlite colonies are contained in more than one ferrite grain. For example, in Fig. 16, the pearlite colony is associated with ferrite grains 1 to 3. Lamellar pearlite colonies were observed occasionally (an example is shown at C in Fig. 17). Similar microstructures have been documented in as-received temper rolled steels [1]. These observations may be explained if partial reaustenitization occurs concurrently with recrystallization of ferrite. This latter point is discussed in more detail in Section 4.2.

4. Discussion

4.1. Crack formation

The results presented in Section 3.2 revealed that massive cementite films at ferrite–ferrite and ferrite–pearlite interfaces were fractured by brittle cracking for all percentage reductions. The cracks develop since the interface between ferrite and cementite acts as a barrier to dislocation flow, hence, dislocations pile up at the interfaces, resulting in a stress concentration [4]. If the stress exceeds the cohesive strength of the interface, a crack may initiate to accommodate the stress and propagate into the cementite, thereby promoting brittle fracture. The crack does not propagate appreciably into the neighbouring proeutectoid ferrite grains since the ease of plastic deformation in the ferrite grains tends to blunt the propagation of the crack into the ferrite [5, 6]. In contrast, cracks at massive cementite films at ferrite–pearlite interfaces can propagate into the pearlitic colony (see Figs 5 and 6). This is most probably due to the fact that the pearlitic ferrite is more plastically constrained compared with the proeutectoid ferrite.

For massive cementite films, brittle cracking is predominant. However, ductile cracking by necking of cementite occurs occasionally at thin cementite films. This latter observation is consistent with the results of other investigators [7–9] who suggested that ductile cracking occurs at relatively thin cementite precipitates.

During the course of this investigation, kinking of cementite lamellae and shear cracking have been observed. The mechanism for kinking of cementite lamellae is the same as that described elsewhere [10, 11] and suggests that the lamellae can be plastically deformed. Cracking of cementite lamellae has been studied extensively by many investigators

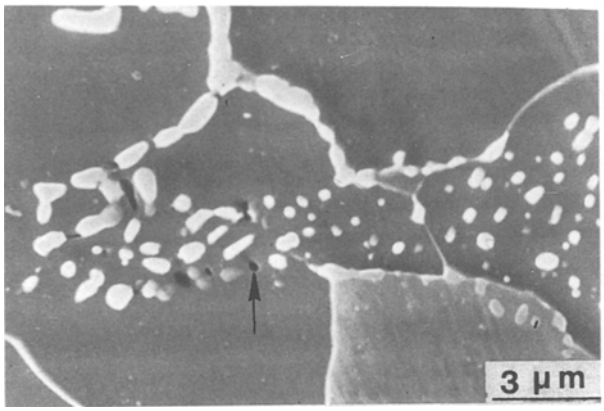

Figure 15 Spheroidization of fractured cementite and growth of cavities from cracks (70% cold rolling plus annealing for 25 min at 700° C, steel B).

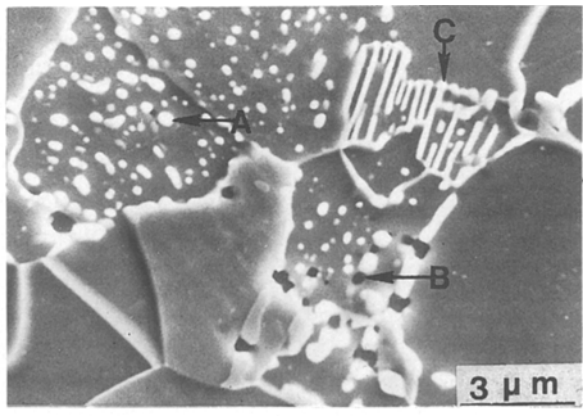

Figure 17 Spheroidized cementite and cavities together with a lamellar pearlite colony (70% cold rolling plus annealing for 3 min at 740° C, steel B).

[6, 11–18], and it is considered generally that coarse and fine pearlites deform in a different manner; the former deforms inhomogeneously, resulting in shear cracking [6, 11–18] whilst the latter deforms in a relatively homogeneous manner, resulting in ductile cracking by necking of the cementite lamellae [6, 15, 16, 18]. Our results are consistent with the above, since the pearlite colonies contained "coarse cementite" and shear cracking of the pearlite cementite occurred (Fig. 5). It has been reported [6, 15, 17] that the cracking of pearlite leads to cleavage cracking of the adjacent proeutectoid ferrite grains, however, cleavage cracks in proeutectoid ferrite were not found in this investigation. This is most probably due to the fact that shear cracks in the pearlite colonies did not traverse the whole colony. It is interesting to note that cavitation in the pearlitic ferrite was associated with shear cracking of the cementite lamellae (e.g., arrowed B in Fig. 5), however, cavitation in the pearlitic ferrite and the adjacent cementite lamellae occurs only infrequently (e.g., at C in Fig. 5). This is consistent with the work of Porter *et al.* [16] who showed that small cavities could grow by ductile rupture of the ferrite and link up through the gap between fractured cementite lamellae.

Cavitation also occurred in the proeutectoid ferrite at:

(1) the proeutectoid ferrite–grain boundary cementite film interfaces (e.g. see Fig. 2).

(2) the pearlite–proeutectoid ferrite interfaces (see Fig. 5) and

(3) fragmented cementite films (Fig. 2).

These results are consistent with previous studies [16, 19–23] in that cavities nucleate at the interface between cementite and the matrix and between fractured cementite. The reason for the occurrence of cavities at sites 1 and 2 above, is similar to that discussed for cavitation in the pearlitic ferrite: ductile rupture of the ferrite occurs due to the concentration of plastic strains [19]. Cavitation at site 3 has been discussed by Porter *et al.* [16] and Alexander and Bernstein [18] for the case of failure within pearlite.

4.2. Cavity formation

As shown in Section 3.2, the cracks which were produced by cold rolling developed into cavities during annealing. Similarly, the fragmented cementite particles spheroidized during annealing at both 700 and 740° C.

At 700° C, the development of cracks into cavities most likely occurs during the recovery and recrystallization stages. It is expected that excess vacancies which were created by cold rolling diffuse to the cracks which develop into cavities [24, 25]. It has been suggested [26–30] that the driving force for the diffusion of vacancies is provided by pre-strain. In addition, free dislocations, subboundaries, and grain boundaries will provide easy diffusion paths for the vacancies. Cavity growth will also be enhanced since the recrystallizing interface will provide a short-circuit diffusion path. Furthermore, spheroidization of the fragmented cementite lamellae will occur rapidly during both recovery and recrystallization for the same reasons outlined above.

Cavity formation at 740° C is expected to be similar to that at 700° C except that both recrystallization and partial reaustenitization occur during cavity growth. The effect of partial reaustenitization of the final microstructure is complex in that studies on intercritical annealing of the cold rolled steels at 740° C for 3 min [31] revealed that pearlite dissolution was not complete. It is likely that the passage of the austenite interface through the pearlite colony could assist in the coarsening of the cavities. In addition, those areas which did transform to austenite should revert to a lamellar pearlitic structure during subsequent cooling to room temperature. Conversely, those pearlitic regions which did not transform to austenite but were recrystallized, would retain the spheroidized cementite morphology developed during the anneal. This could account for the observation of lamellar pearlite in certain areas (e.g., at C in Fig. 17), whereas other regions only contain spheroidized cementite (e.g., Fig. 16 and at A in Fig. 17).

5. Conclusions

The conclusions are as follows.

(1) The pearlitic regions and the massive cementite films in the hot rolled products were fragmented by cold rolling.

(2) Fracture of the massive films at ferrite–ferrite and ferrite–pearlite interfaces occurred in a brittle manner while the small and discrete cementite precipitates did not show any evidence for brittle cracking, however, some of these latter particles necked down leading to ductile failure.

(3) The interface between ferrite and cementite is the nucleation site for the brittle cracks. These cracks form due to the stress concentrations which are created by dislocation pile-ups.

(4) The cracks rarely propagate into the adjacent proeutectoid ferrite grains, but sometimes advance into the pearlitic colonies.

(5) Fracture of pearlitic cementite normally occurs by shear cracking. Plastic deformation of the cementite lamellae by kinking was a rare occurrence.

(6) The cracks which are associated with cementite gradually develop into cavities during subsequent annealing.

(7) The growth of the cavities is most probably achieved by a short-circuit diffusion of excess vacancies driven by pre-strains, but can be facilitated by recrystallization and reaustenitization.

Acknowledgements

The authors wish to acknowledge the American Iron and Steel Institute for their financial support. Dr G. Ludkovsky of Inland Steel is thanked for providing the specimen materials.

References

1. J-W. LEE and P. R. HOWELL, *J. Mater. Sci.* submitted.
2. *Idem, ibid.* **22** (1987) 3631.
3. A. QUERALES and J. G. BYRNE, *Met. Trans.* **11A** (1980) 255.
4. E. SMITH and J. J. BARNBY, *Met. Sci. J.* **1** (1967) 1.
5. K. W. BURNS and F. B. PICKERING, *J. Iron Steel Inst.* **202** (1964) 899.

6. A. R. ROSENFIELD, E. VOTAVA and G. T. HAHN, *Trans. ASM* **61** (1968) 807.
7. T. C. LINDLEY, G. OATES and C. E. RICHARDS, *Acta Metall.* **18** (1970) 1127.
8. J. GURLAND, *ibid.* **20** (1972) 735.
9. G. LANGFORD, *Met. Trans.* **8A** (1977) 861.
10. U. LINDBERG, *Trans. ASM* **61** (1968) 500.
11. L. E. MILLER and G. C. SMITH, *J. Iron Steel Inst.* **208** (1970) 998.
12. J. T. BARNBY and M. R. JOHNSON, *Met. Sci. J.* **3** (1969) 155.
13. J. GIL SAVILLANE, *Mater. Sci. Eng.* **21** (1975) 221.
14. A. INOUE, T. OGURA and T. MASUMOTO, *Trans. Jpn Inst. Met.* **17** (1976) 149.
15. Y. OHMORI and F. TERASAKI, *Trans. Iron Steel Inst. Jpn* **16** (1976) 561.
16. D. A. PORTER, K. E. EASTERLING and G. D. W. SMITH, *Acta Metall.* **16** (1978) 1405.
17. Y. J. PARK and I. M. BERNSTEIN, *Met. Trans.* **10A** (1979) 1653.
18. D. J. ALEXANDER and I. M. BERNSTEIN, in "Phase Transformations in Ferrous Alloys", edited by A. R. Marder and J. I. Goldstein (TMS-AIME, Warrendale, Pennsylvania, 1983) p. 243.
19. J. GURLAND and J. PLATEAU, *Trans. ASM* **56** (1963) 442.
20. D. A. CURRY and P. L. PRATT, *Mater. Sci. Eng.* **37** (1979) 223.
21. J. R. FISHER and J. GURLAND, *Met. Sci.* **15** (1981) 185.
22. A. MELANDER and K. OLSSON, *Met. Tech.* **10** (1983) 424.
23. Y. W. SHI and J. T. BARNBY, *Int. J. Fract.* **25** (1984) 143.
24. J. N. GREENWOOD, *J. Iron Steel Inst.* **176** (1954) 268.
25. R. W. BALLUFFI and L. L. SEIGLE, *Acta Metall.* **3** (1955) 170.
26. D. H. HULL and R. E. RIMMER, *Phil. Mag.* **4** (1953) 673.
27. B. F. DYSON and D. E. HENN, *J. Microscosc.* **97** (1973) 165.
28. B. F. DYSON, *Can. Met. Quart.* **13** (1974) 237.
29. M. KIKUCHI and J. R. WEERTMAN, *Scripta Metall.* **14** (1980) 797.
30. M. KIKUCHI, K. SHIOZAWA and J. R. WEERTMAN, *Acta Metall.* **29** (1981) 1747.
31. J-W. LEE and P. R. HOWELL, unpublished research, The Pennsylvania State University.

Received 19 June
and accepted 22 November 1989